Long-Range Phase Order in Two Dimensions under Shear Flow

Hiroyoshi Nakano,[1] Yuki Minami,[2] and Shin-ichi Sasa[1]
[1]*Department of Physics, Kyoto University, Kyoto 606-8502, Japan*
[2]*Department of Physics, Zhejiang University, Hangzhou 310027, China*

(Received 1 December 2020; accepted 31 March 2021; published 23 April 2021)

We theoretically and numerically investigate a two-dimensional O(2) model where an order parameter is convected by shear flow. We show that a long-range phase order emerges in two dimensions as a result of anomalous suppression of phase fluctuations by the shear flow. Furthermore, we use the finite-size scaling theory to demonstrate that a phase transition to the long-range ordered state from the disordered state is second order. At a transition point far from equilibrium, the critical exponents turn out to be close to the mean-field value for equilibrium systems.

DOI: 10.1103/PhysRevLett.126.160604

Introduction.—Nature exhibits various types of long-range order such as crystalline solids, liquid crystals, ferromagnets, and Bose-Einstein condensation. Whereas they are ubiquitous in the three-dimensional world, some types of long-range order associated with a continuous symmetry breaking are forbidden in two dimensions by the Mermin-Wagner theorem [1–3]. The representative example of this theorem is that there is no long-range phase order in two dimensions.

Recently, the long-range phase order out of equilibrium has attracted much attention. A stimulating example is the characteristic "flocking" behavior among living things such as birds and bacteria. According to extensive numerical simulations of a simple model proposed by Vicsek *et al.* [4], the "flocking" behavior was identified with the spontaneous emergence of the phase order in self-propelled polar particle systems—it is often called the polar order [5]. A remarkable feature here is that it occurs even in two dimensions [6–11] even though it is prohibited for equilibrium systems by the Mermin-Wagner theorem [12]. This phenomenon was also observed in the two-temperature conserved XY model [13,14]. It is now accepted that the long-range phase order can exist even in two dimensions for some nonequilibrium systems with short-range interactions.

The aim of this Letter is to clarify how the long-range phase order emerges in two dimensions under a small nonequilibrium perturbation to equilibrium systems. We study a two-dimensional O(2) model with short-range interaction. For equilibrium O(2) models, the dimension $d = 2$ is marginal; specifically, the long-range phase order is broken by thermal fluctuations for $d \leq 2$ but is stable for $d > 2$ [15–18]. Here, we impose infinitesimal shear flow on such a system and drive it into a nonequilibrium steady state. We then ask whether long-range phase order appears in the externally driven system. This Letter shows that the answer is yes and investigates its origin.

There is a long history of studying phase transitions driven by external nonequilibrium forces. Well-studied examples are related to the Ising universality class, e.g., critical fluids, binary mixtures, and lattice gases [19–24]. The phase transition under shear flow was one of the topics examined in this context [25–33]. In a seminal study, Onuki and Kawasaki performed the renormalization group analysis of the sheared critical fluids [25]. Recently, some groups studied the related systems by using Monte Carlo simulations [29,31–33].

Regarding externally driven systems with continuous symmetry, the main focus has been on three-dimensional phenomena such as an isotropic-to-lamellar transition of block copolymer melts [34–37], an isotropic-to-nematic transition of liquid crystals [38–43], a nematic-to-smectic transition of liquid crystals [44–46], a crystallization of colloidal suspensions [47,48], and a spinodal decomposition of a large-N limit model [49,50]. To our knowledge, the main question of this Letter has been never addressed before.

The key point of our study is to argue the stability of the long-range phase order in terms of the infrared divergence [51]. For the equilibrium O(2) model, the correlation function of the phase fluctuation behaves as $|\boldsymbol{k}|^{-2}$ where $\boldsymbol{k}$ represents the wave number. This fluctuation causes the logarithmic divergence of the real-space correlation function in the limit of large system size and breaks the ordered state. Therefore, if stable long-range phase order appears under the shear flow, this logarithmic divergence must be removed by the flow effects. In this Letter, we theoretically demonstrate that the shear flow anomalously suppresses the phase fluctuation from k_x^{-2} to $|k_x|^{-2/3}$, where the x direction is defined as parallel to the flow. This new phase fluctuation is small enough to remove the divergence. Furthermore, by performing finite-size scaling analysis, we numerically show that the phase transition to the ordered state from the disordered state is second order. We also discuss our simulation result in the context of the previous results obtained for the sheared Ising model.

Model.—Let $\boldsymbol{\varphi}(\boldsymbol{r},t) = (\varphi_1(\boldsymbol{r},t), \varphi_2(\boldsymbol{r},t))$ be a two-component real order parameter defined on a two-dimensional region $[0, L_x] \times [0, L_y]$. The order parameter is convected by the steady uniform shear flow with a velocity $\boldsymbol{v}(\boldsymbol{r}) = (\dot{\gamma} y, 0)$, where $\dot{\gamma} \geq 0$ without loss of generality. The dynamics is given by the time-dependent Ginzburg-Landau model

$$\left[\frac{\partial}{\partial t} + \boldsymbol{v} \cdot \nabla\right] \varphi_a = -\Gamma \frac{\delta \Phi[\boldsymbol{\varphi}]}{\delta \varphi_a} + \eta_a, \tag{1}$$

$$\langle \eta_a(t,\boldsymbol{r}) \eta_b(t',\boldsymbol{r}') \rangle = 2\Gamma T \delta_{ab} \delta(t-t') \delta(\boldsymbol{r}-\boldsymbol{r}'), \tag{2}$$

where the Landau free energy $\Phi[\boldsymbol{\varphi}]$ is given by the standard φ^4 model

$$\Phi[\boldsymbol{\varphi}] = \int d^2\boldsymbol{r} \left[\frac{\kappa}{2} \sum_{a=1}^{2} (\nabla \varphi_a)^2 + \frac{r}{2} |\boldsymbol{\varphi}|^2 + \frac{u}{4} (|\boldsymbol{\varphi}|^2)^2\right]. \tag{3}$$

Here, T is the temperature of the thermal bath, and it is chosen independently of r.

The left-hand side of Eq. (1) represents the rate of change following the flow. We stress that the convection term does not break the rotational symmetry in the order-parameter space. Furthermore, we note that in equilibrium our model is reduced to "model A" in the classification of Hohenberg and Halperin [52,53]. Because the steady-state distribution of $\boldsymbol{\varphi}$ is given by the canonical ensemble, the system exhibits quasi-long-range order instead of long-range order [16,54].

Phase fluctuation in the low-temperature limit.—The state realized at $T = 0$ is given by minimizing the Landau free energy $\Phi[\boldsymbol{\varphi}]$. For $r < 0$, we have the ordered solution $\bar{\boldsymbol{\varphi}} = (\sqrt{-r/u}, 0)$, where we choose the direction of ordering as $\boldsymbol{n} = (1, 0)$. In equilibrium, this ordered state is broken at finite temperature $T > 0$. Here, we study how the shear flow suppresses the equilibrium fluctuations and stabilizes the ordered state in the low-temperature limit.

To analyze the fluctuations around $\bar{\boldsymbol{\varphi}}$, we transform the field variable as $\boldsymbol{\varphi}(\boldsymbol{r},t) = (\sqrt{-r/u} + A(\boldsymbol{r},t))(\cos\theta(\boldsymbol{r},t), \sin\theta(\boldsymbol{r},t))$, where $A(\boldsymbol{r},t)$ is the amplitude fluctuation and $\theta(\boldsymbol{r},t)$ the phase fluctuation. The phase fluctuation corresponds to the gapless mode associated with O(2) symmetry breaking [55–57]. Therefore, we study the phase fluctuation below. Because the thermal fluctuations become sufficiently small in the low-temperature limit, we can neglect the periodicity of $\theta(\boldsymbol{r},t)$ and describe its dynamics within the linear approximation as

$$\left[\frac{\partial}{\partial t} - \dot{\gamma} k_x \frac{\partial}{\partial k_y} + \Gamma \kappa |\boldsymbol{k}|^2\right] \tilde{\theta}(\boldsymbol{k},t) = \tilde{\eta}_2(\boldsymbol{k},t), \tag{4}$$

where $\tilde{\theta}(\boldsymbol{k},t)$ is the Fourier transform of $\theta(\boldsymbol{r},t)$. The equal-time correlation function $C_{\theta\theta}(\boldsymbol{k})$ in the steady state is defined by $\langle \tilde{\theta}(\boldsymbol{k},t) \tilde{\theta}(\boldsymbol{k}',t) \rangle = C_{\theta\theta}(\boldsymbol{k}) \delta(\boldsymbol{k}+\boldsymbol{k}')$, where $\langle \cdots \rangle$ represents the average in the steady state. From Eq. (4), $C_{\theta\theta}(\boldsymbol{k})$ is formally solved as [58]

$$C_{\theta\theta}(\boldsymbol{k}) = T\Gamma \int_0^\infty ds e^{-\Gamma\kappa(s|\boldsymbol{k}|^2 + \frac{1}{2}\dot{\gamma} s^2 k_x k_y + \frac{1}{12}\dot{\gamma}^2 s^3 k_x^2)}. \tag{5}$$

For $\dot{\gamma} = 0$, Eq. (5) is immediately integrated as $C_{\theta\theta}(\boldsymbol{k}) = T|\boldsymbol{k}|^{-2}/\kappa$. In two dimensions, the $|\boldsymbol{k}|^{-2}$ mode leads to the logarithmic divergence of the real-space correlation function and destroys the long-range order.

For $\dot{\gamma} > 0$, the asymptotic behavior of Eq. (5) for small $\boldsymbol{k}$ is calculated as

$$C_{\theta\theta}(\boldsymbol{k}) \simeq \frac{T}{c_0(\sqrt{\kappa}\dot{\gamma}|k_x|/\Gamma)^{\frac{2}{3}} + \kappa |\boldsymbol{k}|^2}, \tag{6}$$

where $c_0 \simeq 2.04$. The shear flow stretches the fluctuations along the x axis, which induces the anisotropic term $(\sqrt{\kappa}\dot{\gamma}|k_x|/\Gamma)^{2/3}$ in Eq. (6). Because the exponent $2/3$ of this term is smaller than 2, the equilibrium fluctuations are suppressed so that the logarithmic divergence in two dimensions is removed. Therefore, the fluctuations under shear flow do not break the long-range phase order for sufficiently low temperatures.

We also observe the exponent $2/3$ beyond the linear regime. To this end, we numerically solve the full equation, Eq. (1), and calculate the structure factor, defined by $\langle \boldsymbol{\varphi}(\boldsymbol{k}) \cdot \boldsymbol{\varphi}(\boldsymbol{k}') \rangle = S(\boldsymbol{k}) \delta(\boldsymbol{k}+\boldsymbol{k}')$. Figure 1 plots $S^{-1}(\boldsymbol{k})$ for $\Gamma = T = u = 1.0$, $\kappa = 0.5$, $\dot{\gamma} = 0.1$, and $r = -3.01$, where we have the long-range ordered state as explained below. From this figure, we find that the k_x dependence of $S^{-1}(k_x, k_y = 0)$ crosses over from $|k_x|^{-2/3}$ to k_x^{-2}. This behavior qualitatively agrees with the linearized model, Eq. (6).

We note that the length scale $l \equiv \sqrt{\kappa\Gamma/\dot{\gamma}}$ governs the crossover behavior. Because $l \to \infty$ in the equilibrium limit $\dot{\gamma} \to +0$, the order of the two limits $\boldsymbol{k} \to \boldsymbol{0}$ and $\dot{\gamma} \to +0$ cannot be exchanged. This observation leads to the result that the fractional mode $|k_x|^{-2/3}$ stabilizes the long-range order even when $\dot{\gamma} \to +0$.

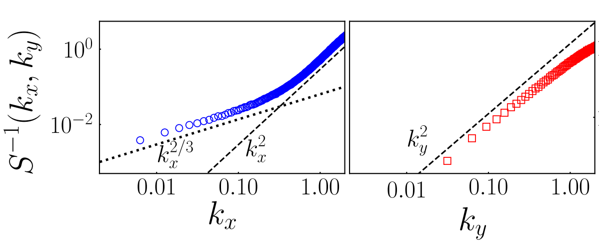

FIG. 1. Structure factor in ordered state. Left: $S^{-1}(k_x, k_y = 0)$ versus k_x. Right: $S^{-1}(k_x = 0, k_y)$ versus k_y.

Finite-size scaling analysis.—We carry out a finite-size scaling analysis to show further evidences of long-range order in the presence of shear flow. Because the finite-size scaling theory in isotropic systems is modified by the anisotropy of shear flow [32], we give an overview below of the finite-size scaling theory in the sheared system. Essentially the same analysis has been used for driven lattice gases [21–23,80].

The finite-size scaling theory is constructed on the basis of the scaling invariance at the second-order phase transition point. The scaling invariance is mathematically expressed by two relations. The first one is written using a free energy $F(\tau, h, L_x^{-1}, L_y^{-1}; \dot{\gamma})$ in the finite-size system, where $\tau = (r - r_c)/r_c$ is the dimensionless distance from the transition point r_c, and h is the external field coupled with $\hat{m} = |\int d^2\boldsymbol{r}\boldsymbol{\varphi}(\boldsymbol{r})|/L_x L_y$. Then, the scaling invariance of the free energy near the critical point is given by the scaling relation

$$F(\tau, h, L_x^{-1}, L_y^{-1}; \dot{\gamma}) = F(b^{z_\tau}\tau, b^{z_h}h, b^{z_x}L_x^{-1}, bL_y^{-1}; \dot{\gamma}) \quad (7)$$

for any $b > 0$, where the three scaling dimensions z_τ, z_h, and z_x are introduced. The second relation is that any quantity $\langle A\rangle_{h=0}$ in the absence of an external field can be expressed in terms of the correlation lengths ξ_x and ξ_y as

$$\langle A\rangle_{h=0}(L_x^{-1}, L_y^{-1}, \tau; \dot{\gamma}) = L_x^{w_A}\mathcal{A}\left(\frac{\xi_x}{L_x}, \frac{\xi_y}{L_y}; \dot{\gamma}\right), \quad (8)$$

where w_A is a constant and $\mathcal{A}$ is a scaling function.

All the critical exponents are expressed by combinations of the three scaling dimensions: z_τ, z_h, and z_x [58]. For example, the critical exponents ν_x and ν_y, characterizing the divergence of the correlation length (i.e., $\xi_i \sim |\tau|^{-\nu_i}$), are expressed as $\nu_x = z_x/z_\tau$ and $\nu_y = 1/z_\tau$. The exponent β, characterizing the onset of magnetization slightly below the critical point (i.e., $\langle\hat{m}\rangle_{h=0} \sim |\tau|^\beta$), is given by $\beta = -\tilde{z}_h/z_\tau$, where we have introduced $\tilde{z}_h \equiv z_h - (1 + z_x)$.

We note that z_x characterizes the anisotropy of the divergence of the correlation length because it is rewritten as ν_x/ν_y. Actually, the anisotropy of the shear flow makes $z_x \neq 1$. This can be immediately confirmed from the theoretical analysis of the linearized model by dropping the φ^4 term from Eq. (3). This model is well-defined for $r > 0$ and exhibits a singular divergence as $r \to +0$. From a similar calculation as the phase fluctuations in the low-temperature limit, we obtain $\nu_x = 3/2$ and $\nu_y = 1/2$, and then z_x is given by $z_x = \nu_x/\nu_y = 3$. Thus, it is natural to introduce $z_x \neq 1$ in the presence of the shear flow.

Now, we show that the finite-size scaling theory works well for our model using numerical simulations. Below, we fix $\Gamma = T = u = 1.0$ and $\kappa = 0.5$ and treat $\dot{\gamma}$ and r as control parameters. From Eqs. (7) and (8), we can derive the system-size dependence of the nth moment of magnetization as

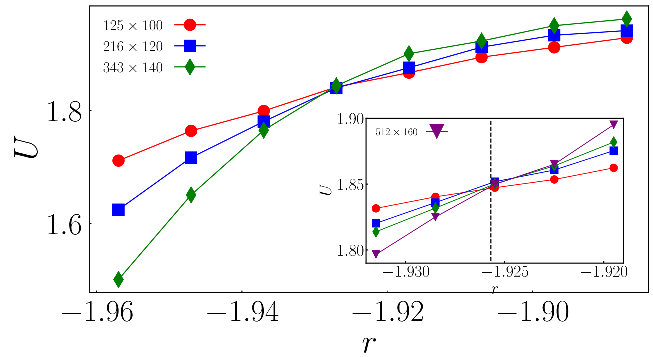

FIG. 2. Binder parameter U as a function of r for $\dot{\gamma} = 5.0$. Inset: enlargement of the intersection point. The error bars of the data are in the order of the point sizes.

$$\langle\hat{m}^n\rangle_{h=0}(L_x^{-1}, L_y^{-1}, \tau; \dot{\gamma}) = L_y^{\tilde{z}_h n}\mathcal{M}_n(L_y^{z_\tau}\tau, L_y^{z_x}L_x^{-1}; \dot{\gamma}). \quad (9)$$

The Binder parameter, defined by $U \equiv \langle\hat{m}^4\rangle_{h=0}/\langle\hat{m}^2\rangle_{h=0}^2$, satisfies

$$U(L_x^{-1}, L_y^{-1}, \tau; \dot{\gamma}) = \mathcal{U}(L_y^{z_\tau}\tau, L_y^{z_x}L_x^{-1}; \dot{\gamma}). \quad (10)$$

This equation means that all curves of the Binder parameter with different L_x values intersect at a unique point when $L_y^{z_x}L_x^{-1}$ is fixed. In Fig. 2, we plot the numerical result for the Binder parameter U for $\dot{\gamma} = 5.0$. We have assumed $z_x = 3$ with reference to the linearized model and chosen the system size as $L_x = 125$, 216, 343, and 512 under the condition $L_y = 20L_x^{1/3}$. This figure shows the existence of the unique intersection point as expected.

According to the finite-size scaling relations Eqs. (9) and (10), the magnetization $\langle\hat{m}\rangle_{h=0}$ and the Binder parameter U can be expanded as power series near the critical point:

$$\langle\hat{m}\rangle_{h=0} = L_y^{\tilde{z}_h}\sum_{n=0}^{N} C_n^m(L_y^{z_x}L_x^{-1})L_y^{z_\tau n}\tau^n, \quad (11)$$

$$U = \sum_{n=0}^{N} C_n^u(L_y^{z_x}L_x^{-1})L_y^{z_\tau n}\tau^n, \quad (12)$$

where C_n^m and C_n^u are expansion coefficients dependent on $L_y^{z_x}L_x^{-1}$. By fitting the simulation data to these expansions, we determine the critical point r_c and the scaling exponent $(\tilde{z}_h, z_\tau)$. In particular, we use the data in the region $-1.930 < r < -1.920$ and perform simultaneous fitting of the two quantities $\langle\hat{m}\rangle_{h=0}$ and U to Eqs. (11) and (12) with $N = 2$; we obtain $r_c = -1.9257 \pm 0.0002$, $z_\tau = 2.05 \pm 0.11$, and $\tilde{z}_h = -0.983 \pm 0.026$. The validity of these fittings is shown in Fig. 3, which is the scaled plot of the two quantities $\langle\hat{m}\rangle_{h=0}$ and U. The scaled data for the different system sizes overlap, verifying the finite-size scaling relations Eqs. (11) and (12). It is noteworthy that the existence of the universal curve provides an evidence of

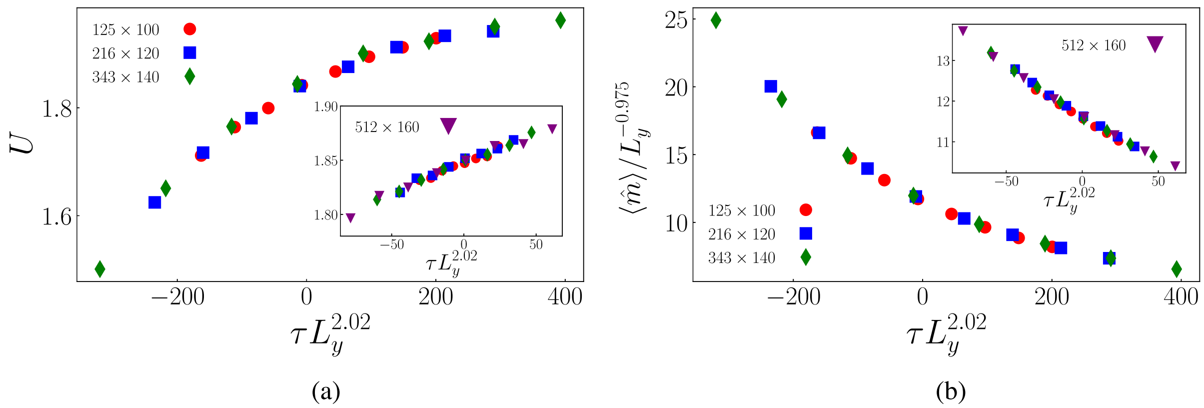

FIG. 3. Finite-size scaling plot for $\dot{\gamma} = 5.0$. (a) U versus $\tau L_y^{z_\tau}$. (b) $\langle \hat{m} \rangle_{h=0} / L_y^{\tilde{z}_h}$ versus $\tau L_y^{z_\tau}$. In both figures, the inset is an enlargement of $\tau = 0$. r_c, z_τ, and $\tilde{z}_h$ are fixed at the best-fit value. The error bars of the data are in the order of the point sizes.

$z_x = 3$. We can also perform the consistency check of $z_x = 3$ from the observation of ν_x and ν_y by using the property that z_x is related to the anisotropy of the divergence of the correlation length [58].

From the obtained values of z_τ and $\tilde{z}_h$, the critical exponent β is calculated as $\beta = -\tilde{z}_h / z_\tau = 0.480 \pm 0.029$. This behavior is very similar to the result for the mean-field theory of the φ^4 model in equilibrium. It is consistent with the previous theoretical results for the sheared Ising model [25,30], where the mean-field character is recovered under a sufficiently large shear rate or in the large limit.

Phase diagram.—We apply the above procedure to systems with smaller $\dot{\gamma}$ and show the phase diagram in Fig. 4, where the critical point r_c is plotted as a function of $\dot{\gamma}$. For all $\dot{\gamma}$ values we have examined, the assumption $z_x = 3$ is valid and the long-range phase order exists below r_c. We then ask where $r_c(\dot{\gamma})$ terminates as $\dot{\gamma} \to +0$. To answer this question, we assume that the critical point r_c behaves as a function of $\dot{\gamma}$ in the form

$$r_c(\dot{\gamma}) = D_0 \dot{\gamma}^w + r_c(+0). \tag{13}$$

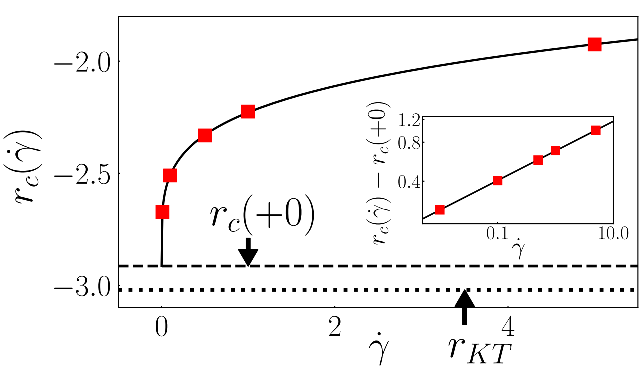

FIG. 4. Critical point r_c as a function of $\dot{\gamma}$. The red points represent the numerical estimation and the black solid line Eq. (13) with the best-fit parameter. Inset: $r_c - r_c(+0)$ versus $\dot{\gamma}$ with a log-log plot.

Note that for the sheared Ising model, this functional form is known to reproduce the behavior of the critical point for small $\dot{\gamma}$ [27,31–33]. By fitting the simulation data to Eq. (13), we obtain the best-fit parameters $r_c(+0) = -2.9139 \pm 0.0151$, $D_0 = 0.685 \pm 0.016$, and $w = 0.228 \pm 0.006$. The corresponding curve is drawn as the black solid one in Fig. 4. The good agreement between the numerical estimation and the best-fit curve confirms the validity of Eq. (13) for our model. This gives the evidence that the long-range phase order is stabilized even under the infinitesimal shear flow. The critical point at the infinitesimal shear rate $\dot{\gamma} \to +0$ is estimated as $r_c(+0) = -2.9139 \pm 0.0151$.

Discussion.—We remember that our model exhibits the Kosterlitz-Thouless transition in equilibrium. The transition point is estimated to be $r_{\mathrm{KT}} = -3.0204 \pm 0.0087$ [3]. Then, our results show that there exists a slight deviation between $r_c(+0)$ and r_{KT}. We here discuss two possible scenarios. The first one is that this deviation disappears by using the data at smaller $\dot{\gamma}$ for larger systems. Actually, for the two-dimensional Ising model [31,32] and the three-dimensional critical fluid [27], $r_c(\dot{\gamma})$ terminates at the equilibrium transition point as $\dot{\gamma} \to +0$. As the second scenario, this deviation may remain for larger systems because the long-wavelength fluctuations ($|k_x| < 2\pi/l$) are drastically altered even when $\dot{\gamma} \to +0$ (see Fig. 1). Which scenario is correct is left for future study.

Another question for small $\dot{\gamma}$ is about the critical exponent β. Our simulation showed that for $\dot{\gamma} = 0.5$, β agrees well with the mean-field value as in the case of $\dot{\gamma} = 5.0$. In contrast, for $\dot{\gamma} = 0.01$, we obtained $z_\tau = 2.03 \pm 0.30$ and $\tilde{z}_h = -0.579 \pm 0.02$, which correspond to $\beta = 0.285$ [3]. Clearly, there is a large deviation between the observed result and mean-field theory. We do not judge whether this deviation comes from the finite-size effects or remains in the large system-size limit. On a related note, this problem also remains controversial for the sheared Ising model [30–33]. More careful analysis for smaller $\dot{\gamma}$ is necessary.

The phase mode induced by the shear flow, $S(k_x, k_y = 0) \sim |k_x|^{-2/3}$, and the long-range order are two sides of the same coin. The interesting point is that the exponent $2/3$ is numerically observed for all $\dot{\gamma}$ values we have examined, although it is derived without considering the nonlinear interaction of fluctuations. This observation suggests that nonlinear effects are irrelevant for the structure factor in the ordered state. The theoretical verification of this conjecture is left as a future work.

Finally, we discuss possible experiments associated with our result. The model in this Letter gives an ideal description of some experimental systems using liquid undercooled metals [81,82] and magnetic fluids [83]. The liquid undercooled metal is known to exhibit the liquid ferromagnet phase due to short-ranged exchange interactions in three dimensions [81,82]. We expect that the two-dimensional liquid ferromagnet phase can be observed by designing a two-dimensional system [8].

We thank M. Kobayashi for helpful comments on the numerical simulation, D. Nishiguchi for a critical reading of the manuscript, and M. Hongo for stimulating conversations. H. N. and S. S. are supported by KAKENHI (No. 17H01148, No. 19H05795, and No. 20K20425). Y. M. is supported by the Zhejiang Provincial Natural Science Foundation Key Project (Grant No. LZ19A050001) and NSF of China (Grants No. 11975199 and No. 11674283).

[1] N. D. Mermin and H. Wagner, Phys. Rev. Lett. **17**, 1133 (1966).
[2] P. C. Hohenberg, Phys. Rev. **158**, 383 (1967).
[3] N. D. Mermin, Phys. Rev. **176**, 250 (1968).
[4] T. Vicsek, A. Czirók, E. Ben-Jacob, I. Cohen, and O. Shochet, Phys. Rev. Lett. **75**, 1226 (1995).
[5] H. Chaté, Annu. Rev. Condens. Matter Phys. **11**, 189 (2020).
[6] J. Toner and Y. Tu, Phys. Rev. Lett. **75**, 4326 (1995).
[7] J. Toner and Y. Tu, Phys. Rev. E **58**, 4828 (1998).
[8] D. Nishiguchi, K. H. Nagai, H. Chaté, and M. Sano, Phys. Rev. E **95**, 020601(R) (2017).
[9] L. P. Dadhichi, A. Maitra, and S. Ramaswamy, J. Stat. Mech. (2018) 123201.
[10] S. Tanida, K. Furuta, K. Nishikawa, T. Hiraiwa, H. Kojima, K. Oiwa, and M. Sano, Phys. Rev. E **101**, 032607 (2020).
[11] L. P. Dadhichi, J. Kethapelli, R. Chajwa, S. Ramaswamy, and A. Maitra, Phys. Rev. E **101**, 052601 (2020).
[12] H. Tasaki, Phys. Rev. Lett. **125**, 220601 (2020).
[13] K. E. Bassler and Z. Rácz, Phys. Rev. E **52**, R9 (1995).
[14] M. D. Reichl, C. I. Del Genio, and K. E. Bassler, Phys. Rev. E **82**, 040102(R) (2010).
[15] V. Berezinskii, Sov. Phys. JETP **32**, 493 (1971).
[16] J. M. Kosterlitz and D. J. Thouless, J. Phys. C **6**, 1181 (1973).
[17] J. M. Kosterlitz, J. Phys. C **7**, 1046 (1974).
[18] T. Koma and H. Tasaki, Phys. Rev. Lett. **74**, 3916 (1995).
[19] S. Katz, J. L. Lebowitz, and H. Spohn, J. Stat. Phys. **34**, 497 (1984).
[20] H. van Beijeren and L. S. Schulman, Phys. Rev. Lett. **53**, 806 (1984).
[21] J.-S. Wang, K. Binder, and J. L. Lebowitz, J. Stat. Phys. **56**, 783 (1989).
[22] K.-t. Leung, Phys. Rev. Lett. **66**, 453 (1991).
[23] S. Caracciolo, A. Gambassi, M. Gubinelli, and A. Pelissetto, J. Stat. Phys. **115**, 281 (2004).
[24] J. Marro and R. Dickman, *Nonequilibrium Phase Transitions in Lattice Models* (Cambridge University Press, Cambrdige, England, 2005).
[25] A. Onuki and K. Kawasaki, Ann. Phys. (N.Y.) **121**, 456 (1979).
[26] A. Onuki, J. Phys. Condens. Matter **9**, 6119 (1997).
[27] A. Onuki, *Phase Transition Dynamics* (Cambridge University Press, Cambridge, England, 2002).
[28] F. Corberi, G. Gonnella, and A. Lamura, Phys. Rev. Lett. **83**, 4057 (1999).
[29] E. N. M. Cirillo, G. Gonnella, and G. P. Saracco, Phys. Rev. E **72**, 026139 (2005).
[30] A. Hucht, Phys. Rev. E **80**, 061138 (2009).
[31] G. P. Saracco and G. Gonnella, Phys. Rev. E **80**, 051126 (2009).
[32] D. Winter, P. Virnau, J. Horbach, and K. Binder, Europhys. Lett. **91**, 60002 (2010).
[33] S. Angst, A. Hucht, and D. E. Wolf, Phys. Rev. E **85**, 051120 (2012).
[34] M. E. Cates and S. T. Milner, Phys. Rev. Lett. **62**, 1856 (1989).
[35] K. A. Koppi, M. Tirrell, and F. S. Bates, Phys. Rev. Lett. **70**, 1449 (1993).
[36] G. H. Fredrickson, J. Rheol. **38**, 1045 (1994).
[37] A. V. Zvelindovsky, G. J. A. Sevink, and J. G. E. M. Fraaije, Phys. Rev. E **62**, R3063(R) (2000).
[38] P. D. Olmsted and P. Goldbart, Phys. Rev. A **41**, 4578 (1990).
[39] P. D. Olmsted and P. M. Goldbart, Phys. Rev. A **46**, 4966 (1992).
[40] N. Grizzuti and P. L. Maffettone, J. Chem. Phys. **118**, 5195 (2003).
[41] M. P. Lettinga and J. K. G. Dhont, J. Phys. Condens. Matter **16**, S3929 (2004).
[42] E. K. Hobbie and D. J. Fry, Phys. Rev. Lett. **97**, 036101 (2006).
[43] M. Ripoll, P. Holmqvist, R. G. Winkler, G. Gompper, J. K. G. Dhont, and M. P. Lettinga, Phys. Rev. Lett. **101**, 168302 (2008).
[44] P. G. D. Gennes, Mol. Cryst. Liq. Cryst. **34**, 91 (1976).
[45] R. F. Bruinsma and C. R. Safinya, Phys. Rev. A **43**, 5377 (1991).
[46] C. R. Safinya, E. B. Sirota, and R. J. Plano, Phys. Rev. Lett. **66**, 1986 (1991).
[47] S. Butler and P. Harrowell, Nature (London) **415**, 1008 (2002).
[48] M. J. Miyama and S.-i. Sasa, Phys. Rev. E **83**, 020401(R) (2011).
[49] F. Corberi, E. Lippiello, and M. Zannetti, Phys. Rev. E **65**, 046136 (2002).
[50] F. Corberi, G. Gonnella, E. Lippiello, and M. Zannetti, J. Phys. A **36**, 4729 (2003).

[51] N. Goldenfeld, *Lectures on Phase Transitions and the Renormalization Group* (CRC Press, Boca Raton, 2018).
[52] P. C. Hohenberg and B. I. Halperin, Rev. Mod. Phys. **49**, 435 (1977).
[53] G. F. Mazenko, *Nonequilibrium Statistical Mechanics* (John Wiley & Sons, New York, 2008).
[54] R. Gupta and C. F. Baillie, Phys. Rev. B **45**, 2883 (1992).
[55] J. Goldstone, Il Nuovo Cimento (1955–1965) **19**, 154 (1961).
[56] Y. Nambu and G. Jona-Lasinio, Phys. Rev. **122**, 345 (1961).
[57] J. Goldstone, A. Salam, and S. Weinberg, Phys. Rev. **127**, 965 (1962).
[58] See Supplemental Material at http://link.aps.org/supplemental/10.1103/PhysRevLett.126.160604 for detailed analysis of linear fluctuations, which includes Refs. [59–79], for details of the finite-size scaling theory, and for supplemental numerical data.
[59] G. H. Fredrickson, J. Chem. Phys. **85**, 5306 (1986).
[60] F. Corberi, G. Gonnella, and A. Lamura, Phys. Rev. E **66**, 016114 (2002).
[61] H. Wada and S.-i. Sasa, Phys. Rev. E **67**, 065302(R) (2003).
[62] H. Wada, Phys. Rev. E **69**, 031202 (2004).
[63] M. Otsuki and H. Hayakawa, Phys. Rev. E **79**, 021502 (2009).
[64] S. Toh, K. Ohkitani, and M. Yamada, Physica (Amsterdam) **51D**, 569 (1991).
[65] A. Onuki, J. Phys. Soc. Jpn. **66**, 1836 (1997).
[66] K. Debrabant and A. Rößler, Math. Comput. Simul. **77**, 408 (2008).
[67] A. W. Lees and S. F. Edwards, J. Phys. C **5**, 1921 (1972).
[68] J.-S. Wang, J. Stat. Phys. **82**, 1409 (1996).
[69] E. V. Albano and G. Saracco, Phys. Rev. Lett. **88**, 145701 (2002).
[70] C. K. Chan and L. Lin, Europhys. Lett. **11**, 13 (1990).
[71] A. Hucht and S. Angst, Europhys. Lett. **100**, 20003 (2012).
[72] Y. Ozeki, K. Ogawa, and N. Ito, Phys. Rev. E **67**, 026702 (2003).
[73] Y. Ozeki and N. Ito, J. Phys. A **40**, R149 (2007).
[74] M. E. Fisher, M. N. Barber, and D. Jasnow, Phys. Rev. A **8**, 1111 (1973).
[75] T. Ohta and D. Jasnow, Phys. Rev. B **20**, 139 (1979).
[76] H. Weber and P. Minnhagen, Phys. Rev. B **37**, 5986 (1988).
[77] N. Schultka and E. Manousakis, Phys. Rev. B **49**, 12071 (1994).
[78] P. Olsson, Phys. Rev. B **52**, 4526 (1995).
[79] M. Hasenbusch, J. Phys. A **38**, 5869 (2005).
[80] K. Binder and J.-S. Wang, J. Stat. Phys. **55**, 87 (1989).
[81] J. Reske, D. M. Herlach, F. Keuser, K. Maier, and D. Platzek, Phys. Rev. Lett. **75**, 737 (1995).
[82] T. Albrecht, C. Bührer, M. Fähnle, K. Maier, D. Platzek, and J. Reske, Appl. Phys. A **65**, 215 (1997).
[83] M. J. P. Nijmeijer and J. J. Weis, Phys. Rev. Lett. **75**, 2887 (1995).